Supplementary Materials for

Nucleoside reverse transcriptase inhibitors possess intrinsic anti-inflammatory activity

Benjamin J. Fowler, Bradley D. Gelfand, Younghee Kim, Nagaraj Kerur, Valeria Tarallo, Yoshio Hirano, Shoba Amarnath, Daniel H. Fowler, Marta Radwan, Mark T. Young, Keir Pittman, Paul Kubes, Hitesh K. Agarwal, Keykavous A. Parang, David R. Hinton, Ana Bastos-Carvalho, Shengjian Li, Tetsuhiro Yasuma, Takeshi Mizutani, Reo Yasuma, Charles Wright, Jayakrishna Ambati*

* Corresponding author. Email: jamba2@email.uky.edu

This PDF file includes:

Materials and Methods

Supplementary Text

Figs. S1 to S21

Materials and methods

Mice

Ocular animal experiments were in accordance with the Association for Research in Vision and Ophthalmology Statement for the Use of Animals in Ophthalmic and Visual Research. WT C57BL6/J mice were purchased from The Jackson Laboratory and Pannexin-1-deficient mice were obtained from Genentech. For all procedures, anesthesia was achieved by intraperitoneal injection of 100 mg/kg ketamine hydrochloride (Ft. Dodge Animal Health) and 10 mg/kg xylazine (Phoenix Scientific), and pupils were dilated with topical 1% tropicamide (Alcon Laboratories). Fundus imaging of dilated mouse eyes was performed on a TRC-50 IX camera (Topcon) linked to a digital imaging system (Sony). For GVHD experiments, adult female C57BL/6 (B6, H_2K^b) and BALB/c (H_2K^d) mice 8- to 10- weeks old were obtained from Frederick Cancer Research Facility. Mice were maintained in a specific pathogen-free facility, and treated according to an approved animal protocol. Drinking water was supplemented with ciprofloxacin from day –1 to day +14 after total body irradiation (TBI). For liver injury model, LysM-eGFP knock-in mice were a gift from Dr. T. Graf (Albert Einstein University, NY). Animals were maintained in a specific pathogen-free facility at the University of Calgary Animal Resource Centre. Experimental animal protocols used in this study were approved by the University of Calgary Animal Care Committee, and were in compliance with guidelines from the Canadian Council for Animal Care.

Immunolabeling

Mouse RPE/choroid flat mounts were fixed with 4% paraformaldehyde or 100% methanol, stained with antibodies against zonula occludens-1 (ZO-1) and visualized with Alexa594 (Invitrogen). All images were obtained using the Leica SP-5 microscope.

Subretinal injection

Subretinal injections (SRI) (1 μL) in mice were performed using an Ito microsyringe (Ito Corporation). In vivo transfection of plasmids coding for an *Alu* sequence (pAlu) or empty control vector (pNull) was achieved using 10% Neuroporter (Genlantis) as described in (*3*). For oral administration, d4T was mixed with carboxymethylcellulose sodium salt (final 0.5%) delivered once daily by oral gavage at 50 or 150 mg/kg. CMC alone was used as vehicle control. For intraperitoneal injection (subretinal *Alu* experiment), AZT was dissolved in UPS-grade 1x PBS (Gibco) was administered twice daily (50 mg/kg/administration; vs. control PBS). Me-d4T was dissolved in 100% DMSO and administered twice daily (25 mg/kg/administration; vs. control DMSO). For both oral gavage and intraperitoneal administration, NRTIs (or control) were delivered starting one day before SRI until six days after SRI.

In vitro transcribed Alu RNA

Alu RNA was synthesized from a linearized plasmid containing a consensus Alu Y sequence with an adjacent 5' T7 promoter, subjected to AmpliScribe T7 Flash Transcription kit (Epicenter) according to the manufacturer's instructions. Dnase-treated

RNA was purified using MEGAclear (Ambion) and integrity monitored by gel electrophoresis.

Reagents

3TC, AZT, LPS, ATP, and bzATP, were purchased from Sigma. D4T was purchased from Sigma and Selleckchem. MSU, flagellin, and poly dA:dT were purchased from Invivogen.

Western blot

Protein samples were run on 4-20% or 4-12% tris-glycine SDS-PAGE gels, transferred to PVDF membrane (0.2 or 0.45 μm), and blotted with antibodies against Caspase-1 (1:250, Santa Cruz (sc-514) for mouse BMDM and mouse RPE *in vivo* experiments; 1:500, Invitrogen or 1:1000, Abcam for all other experiments); pIRAK4 (1:500, Cell Signaling); Vinculin (1:1,000, Sigma-Aldrich), P2RX7 (1: 1000, Abcam); IL1B (1: 500, Cell Signaling), IL-18 (1:250, Biovision), or Tubulin (1:1000, Sigma). Cells were homogenized in RIPA buffer (Sigma) with protease and phosphatase inhibitors (Roche) or lysed directly in Laemmli buffer (*2*). For RIPA extraction, protein concentrations were determined using a Bradford assay kit (Bio-Rad) with bovine serum albumin as a standard. For analysis of cell culture supernatants, media was collected and centrifuged for 10 minutes at 1500 rpm. The supernatant was concentrated through a 10,000 MWCO column (Sartorius Biotech), or precipitated with 20% TCA at -20 C, washed twice with acetone and dried pellet was resuspended in Laemmli buffer and boiled. Proteins were run on a Novex Tris-glycine 4-20% gel (Invitrogen) and transferred

to Immun-Blot PVDF membranes (Bio-Rad) or Immobilon FL PVDF (Millipore). Primary antibody incubation was performed overnight at 4 °C. Protein loading was assessed by immunoblotting using an anti-Vinculin antibody. Secondary antibodies (Santa Cruz, 1:5000; or LICOR, 680/800 nm IRdyes, 1:20000) were used for 1 hour at room temperature. The signal was visualized using a luminol detection kit (Santa Cruz) and captured on UltraCruz ultraradiography film (Santa Cruz) or using the LICOR Odyssey Imager. Densitometry was performed using ImageJ software (NIH).

Quantitative real-time qPCR

Total DNA was extracted from cells and amplified by real-time quantitative PCR (Applied Biosystems 7900 HT Fast Real-Time PCR system) with Power SYBR green Master Mix. Oligonucleotide primers specific for mouse mtDNA COX1 (F 5' TTC GGA GCC TGA GCG GGA AT 3'; R 5' ATG CCT GCG GCT AGC ACT GG 3') were used and normalized to a genomic DNA exon-intron junction (F 5' GTG AGG CGG GCT CCC TGC TG 3'; R 5' CTT CGA ACG CGG AAC GGG ACC 3'). The qPCR cycling conditions were 50 °C for 2 min, 95 °C for 10 min followed by 40 cycles of a two-step amplification program (95 °C for 15 s and 58 °C for 1 min). At the end of the amplification, melting curve analysis was applied using the dissociation protocol from the Sequence Detection system to exclude contamination with unspecific PCR products. Relative expressions of target genes were determined by the $2^{-\Delta\Delta Ct}$ method.

Primary human RPE cell isolation and culture

RPE cells were isolated from human fetal eyes of 18–20 weeks gestation (Novogenixlabs, Los Angeles CA) by soaking the eyes in PBS containing 5% penicillin/streptomycin, cleaning off excess connective tissue, and removing the cornea, lens, vitreous, and retina. The RPE choroidal/scleral tissue was placed in a 2% Dispase solution (Life Technologies, Grand Island, NY) in PBS for 20 min at 37 °C, mixed by pipetting up and down for 30 sec, and filtered by passing through a 70 μm, then a 40 μm filter. RPE cells were recovered by centrifugation and resuspended in Dulbecco's minimum essential medium (DMEM) supplemented with 2 mM L-glutamine, 100 U/mL penicillin, 100 μg/mL streptomycin (VWR International, West Chester, PA) containing at least 25% heat-inactivated fetal bovine serum (FBS; Irvine Scientific, Santa Ana, CA). The cells were first plated on laminin-coated plates until ready to be divided; no further coating was necessary and cells were grown in 10% DMEM. The cells were confirmed to be RPE cells by immunocytochemical positivity for cytokeratin (>95%) and the lack of immunoreactivity for endothelial-cell–specific von Willebrand factor (Dako, Carpinteria, CA) and glial fibrillary acidic protein (Chemicon, Temecula, CA).

Cell culture and transfection experiments

Cell culture of primary human RPE cells was in DMEM with 10% fetal bovine serum (FBS) or 20% FBS (primary mouse RPE cells) with 100 U/ml Penicillin/Streptomycin and 2 mM L-Glutamine, or for ATP/potassium measurements in DMEM without serum. Transfections were performed according to the manufacturers instructions (Lipofectamine 2000, Invitrogen). NRTIs were administered 20 minutes

before *Alu* RNA transfection and added again upon replacement of P/S-containing media at 8 hours. Similarly, ^{10}Panx peptide (Tocris 3348) or scrambled ^{10}Panx control (Tocris 3708) were administered at 240 μM. Primary bone marrow-derived macrophages were isolated, and cultured as described previously (*41*) , and serum starved in 1% FBS-containing Isocove's DMEM overnight prior to LPS stimulation. NRTIs were added 30 minutes prior to LPS stimulation and again 30 minutes prior to activation signal (ATP, nigericin, MSU, flagellin, poly dA:dT). LPS was added at 1000 ng/mL for 3–4 hours prior to ATP/nigericin as previously described (*42*); 500 ng/mL to flagellin (*15*); 200 ng/mL to poly dA:dT (*43*); and 100 ng/mL to MSU (*25*). Cell lysates were collected at 30 minutes after activation signal for ATP (5 mM) and nigericin (20 μM); 6 hours for MSU (250 μg/mL); 4 hours for Flagellin (20 μg/mL transfected with DOTAP) and poly dA:dT (1.5 μg/mL transfected with Lipofectamine). Raji $TK^{-/+}$ cells were cultured in RPMI with 10% FBS. For electrophysiology experiments, human embryonic kidney 293 (HEK293) cells were maintained in Dulbecco's Modified Eagle Medium: Nutrient Mixture F12 (DMEM/F12) supplemented with 10% FBS, 100 U/ml Penicillin/Streptomycin and 2 mM L-Glutamine. Cells were co-transfected with 1 μg plasmid DNA expressing rP2X7 or mP2X7 and 0.1 μg plasmid DNA expressing eGFP using Lipofectamine2000 (Invitrogen, Paisley, UK) according to manufacturer's protocol. 24 hrs after transfection cells were trypsinised and transferred onto sterile poly-L-Lysine (Sigma-Aldrich, Gillingham, UK) coated 13 mm coverslips and incubated overnight prior to the electrophysiology recordings. For lentivirus-GFP experiments, 100 μM d4T or me-d4T was added to HeLa cells two hours before addition of lentivirus-GFP at a MOI of 10. At 24 hours an additional 100 μM d4T or me-d4T was added to cells, and at 48 hours cells were briefly

fixed in 4% PFA before imaging. For cell counting of GFP-positive cells, four fields were chosen at random for each condition, images were processed at the same threshold, and GFP-positive cells were counted using ImageJ.

Northern blot

Total RNA from biotin-UTP *Alu* RNA-transfected cells was extracted using Trizol reagent (Invitrogen). RNA samples were run on 10% TBE-urea gels (BioRad) according to the manufacturers instructions. Samples were transferred and UV cross-linked to a HyBond N+ nylon membrane and blotted for u6 using a biotinylated oligonucleotide probe synthesized by IDT (5' CACGAATTTGCGTGTCATCCTT-Biotin 3'). Blots were developed with the Thermo Pierce chemiluminescent nucleic acid detection kit.

Liquid chromatography and Mass spectrometry

HPLC was run using a 2 Varian ProStar model 210 HPLC solvent delivery module and a Phenomenex Kinetix C-18 column (100 mm x 2.1 mm x 2.6 μM). Solvent compositions were (A): 3 mM Ammonium formate and 10 mM N,N-dimethylhexylamine in H_20; (B): 1:1 acetonitrile:H_2O with 3 mM Ammonium formate and 10 mM N,N-dimethylhexylamine. HPLC mobile phase and flow rate were:

Time (min)	A %	B%	Flow (mL/min)
0	95	5	0.2
3	95	5	0.2
25	40	60	0.2
26	0	100	0.2
29	0	100	0.2
30	95	5	0.2
40	95	5	0.2

Mass Spectrometry was performed on a Varian 1200 L quadrupole MS/MS. Analytes were analyzed with electrospray ionization on negative mode. Cell extracts from Raji $TK^{-/+}$ cells were prepared by adding 40% acetonitrile/20% methanol/20% water to cell pellets, incubation at –20 °C for 15 minutes followed by centrifugation at 4 °C for 5 minutes at 20,000 x g. Two sequential extractions were performed per cell pellet, pooled, and stored at – 80 °C until analysis.

Methoxy-d4T synthesis

Depicted in Supplementary Figure 4.

MitoSOx assay

MitoSox dye was obtained from Invitrogen and used according to the manufacturer's instructions.

ATP assay

Cell culture supernatant was collected from cells and subjected to Enliten ATP assay (Promega) according to manufacturer's instructions.

YO-PRO-1 assay

YO-PRO-1 iodide was from Invitrogen. HEK293 cells stably expressing the human P2X7 receptor were cultured in $G418^+$ DMEM with 10% fetal bovine serum. Cells were trypsinized, and pellets were washed twice in 1x HBSS (without calcium and magnesium). Resuspended cells were plated at 1×10^5 cells/well on a 96 well black-walled cell culture plates spotted with A438079 or d4T to a concentration 64 μM. Cells were incubated at 37 °C and 5% CO_2 for 30 minutes before addition of bzATP (100 μM) for 5 minutes, followed by YO-PRO-1 addition (2.5 μM) after which plates were read immediately for fluorescence (485 ex/530 em) every 30 seconds for 5 minutes in a BioTek Synergy 4 plate reader.

Electrophysiology

Whole-cell patch-clamp recordings were made at room temperature using borosilicate glass pipettes (World Precision Instruments, Sarasota, FL, USA) which had resistances of 3–5 MΩ when filled with a solution containing the following (in mM): 145

NaCl, 10 EGTA and 10 HEPES, with the pH adjusted to 7.3 with NaOH. The recording chamber was continually perfused with extracellular saline solution (ECS) containing (in mM): 147 NaCl, 2 KCl, 1 MgCl2, 2 CaCl2, 10 HEPES and 13 glucose, with the pH adjusted to 7.3 with NaOH. To obtain larger whole-cell currents by relieving divalent cation inhibition of P2X7 receptors (*44*) , 1 mM ATP, 100 μM d4T and 1 mM ATP + 100 μM d4T were made in ECS with low concentrations of divalent cations (ECS-LD) containing (in mM): 147 NaCl, 2 KCl, 0.2 CaCl2, 10 HEPES and 13 glucose, with the pH adjusted to 7.3 with NaOH . Current recordings were made at a holding potential of −60 mV using an Axon Instruments Axopatch Multiclamp 700A amplifier and Digidata 1322A A/D interface (Molecular Devices, Sunnyvale, CA, USA). Agonist applications were made at 90-s intervals. Compounds were applied to patch-clamped cells by means of a rapid perfusion system (RSC-160, Biologic, Claix, France), allowing solution exchange times in the range 20–100 ms.

Bone Marrow Transplant

Bone marrow (BM) cells from B6 mice were harvested and T-cell depleted (T-depleted; anti-CD90 [Thy1.2] microbeads (Miltenyi Biotec). Host allogeneic recipients (BALB/c) were conditioned with TBI of 950 cGy. BALB/c mice were rescued with 10M B6.T-depleted BM (TDBM) cells alone or together with 2.5M bulk T cells ($CD4^+$) from B6.WT mice. Murine recipients that were reconstituted with TDBM and $CD4^+$ T cells were additionally treated for 10 days with either saline or stavudine (twice daily 25 mg/kg/administration) via i.p injections; stavudine was initiated at either day –1 or day 0

of BMT, as indicated in figure legend. Survival and clinical manifestations of GVHD were monitored.

Sterile liver inflammation model

Prior to each experiment, d4T (400 mg/kg) or control saline was administered via jugular vein approximately 20 minutes prior to sterile liver injury. Mice were anaesthetized with a solution containing ketamine hydrochloride (200 mg/kg) and xylazine hydrochloride (10 mg/kg), via intraperitoneal injection, per the University of Calgary Animal Use Protocol. The jugular vein was exposed and cannulated for administration of additional anaesthetic and for administration of the compound or vehicle. Following administration of compound or vehicle, a midline laparotomy was performed and a ~2.5 centimeter diameter section of skin and peritoneum were removed from the ventral surface of the abdomen, exposing the organs of the peritoneum. An electro-cautery probe fitted with a 30 gauge needle bent at a 90° angle was used to induce a single focal injury on the ventral surface of the left lobe of the liver. Two hour recordings at 4x magnification were undertaken, using both green (LysMeGFP^{+} cells) and red (autofluorescence) channels (exposure times of 400 ms respectively). Images were analyzed using ImageJ software and the number of GFP^{+} objects per field of view surrounding the sterile injury site was determined.

Laser-induced choroidal neovascularization

Laser photocoagulation (OcuLight GL, IRIDEX) was performed on both eyes of mice to induce CNV as previously described (*45*). Drugs (d4T or me-d4T) were injected

into the vitreous humor of mice using a 33-gauge double-caliber needle (Ito Corporation) once, immediately after laser injury as previously described. Choroidal angiogenesis volumes were measured by scanning laser confocal microscopy (TCS SP5, Leica) 7 days after injury as previously reported with 0.7% FITC-conjugated Isolectin B4 (Vector) in masked fashion (*45, 46*).

Statistical analysis

Results are expressed as mean ± standard error of the mean (SEM), with p values < 0.05 considered statistically significant. Differences between groups were compared by Mann-Whitney U test, Student's t test, one-way ANOVA with Tukey's post-hoc test, or two-way ANOVA with Student-Newman-Keuls post-hoc test, as appropriate, and two-tailed p values are reported. Survival analysis was performed according to the Kaplan-Meier method and survival curves were compared using log-rank test. Fisher's exact test (two-tailed) was performed for fundus photographs on pAlu vs. pAlu + NRTI groups. Fundus photographs were de-identified and graded in a binary "yes" or "no" readout in terms of RPE degeneration by a retina specialist. Typical induction of RPE degeneration by *Alu* was about 25% of the visible area of the fundus photograph.

Supplementary Text

Author Contributions

B.J.F., B.D.G., Y.K., N.K., V.T., Y.H., S.A., M.R., M.T.Y., K. Pittman, A.B.C., T.Y., T.M., R.Y., and C.W. performed experiments. D.R.H. and K. Parang provided reagents. J.A. and B.J.F. conceived and directed the project, and wrote the paper. All authors had the opportunity to discuss the results and comment on the manuscript.

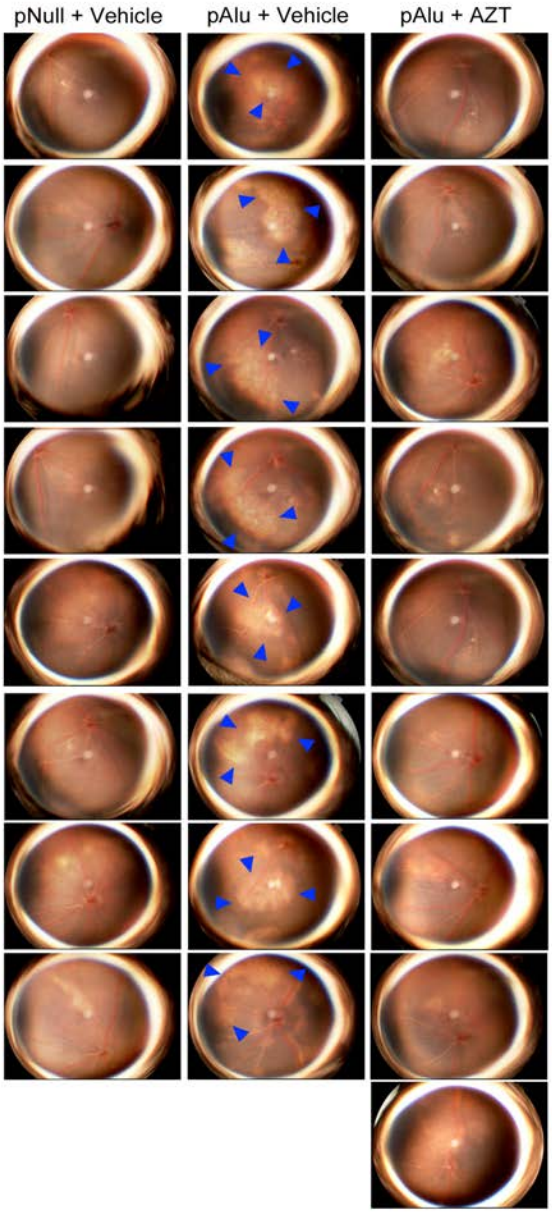

fig. S1. AZT blocks *Alu*-induced RPE degeneration, related to Figure 1B.

Fundus images from wild-type mice given sub-retinal injection of control plasmid (pNull) or *Alu* RNA-expressing plasmid (pAlu). Intraperitoneal AZT (twice daily 50 mg/kg) blocked pAlu-induced RPE degeneration. All fundus images from experiment shown in Fig. 1B.

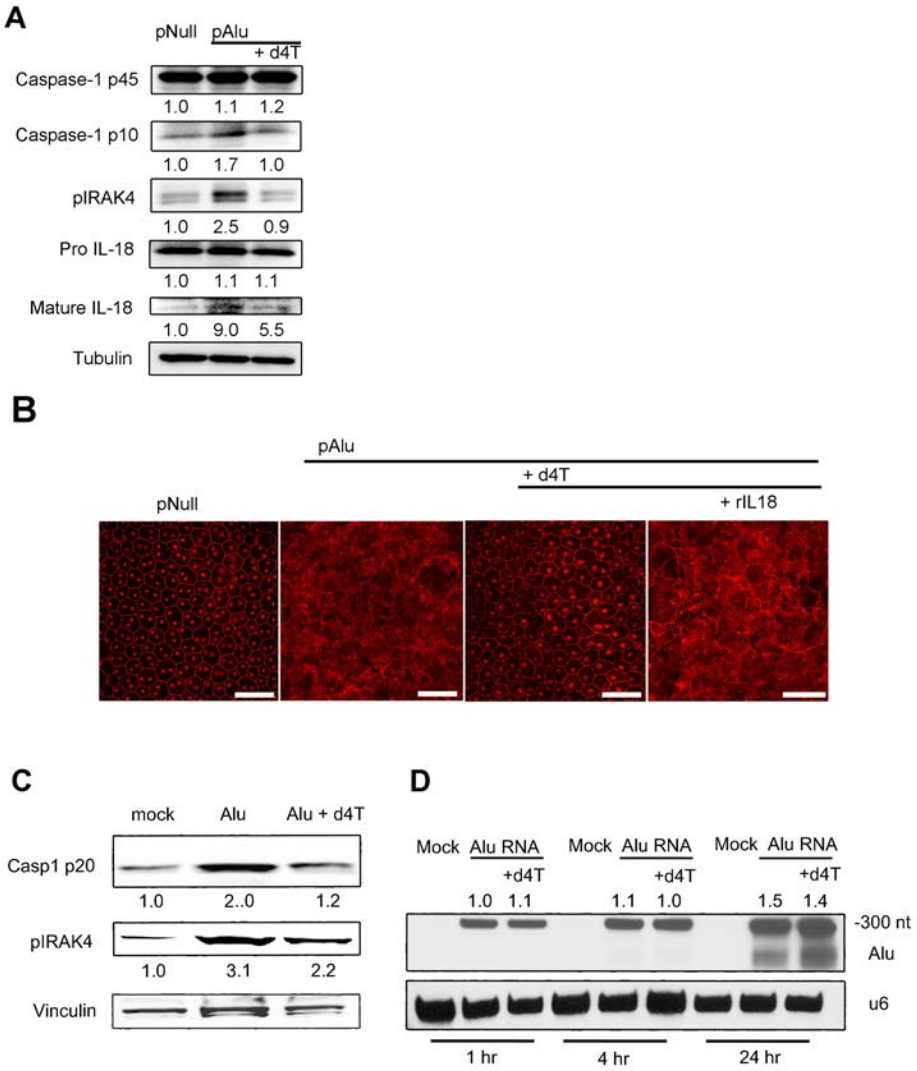

fig. S2. D4T blocks Caspase-1 activation without reducing *Alu* RNA levels, Related to Figure 1.

(A) Western blot of RPE lysates from pNull vs. pAlu-treated mice. Treatment with intraperitoneal d4T (twice daily 50 mg/kg) blocks pAlu-induced Caspase-1 activation (p10), IRAK4 phosphorylation and IL-18 maturation *in vivo*. n = 4. Fold change in densitometry compared to pNull.

(B) Representative RPE flat mounts stained for zonula occludens (ZO-1) showing that intraperitoneal d4T (twice daily 50 mg/kg; related to fig. S2A) blocked pAlu-induced RPE degeneration in 8/8 mice (vs. 1/8 in pAlu + vehicle; $P = 0.001$), which was reversed with addition of subretinal recombinant mouse IL-18 (40 ng; RPE degeneration seen in 7/8 mice; $P = 0.001$). Scale bars 50 μm.

(C) Western blot of Caspase-1 activation (p20 subunit) and IRAK4 phosphorylation in primary mouse RPE cells transfected with *Alu* RNA ± d4T (100 μM). Image representative of n = 4. Fold change in densitometry compared to mock.

(D) Northern blot of biotin-UTP-labeled *Alu* RNA-transfected primary human RPE cells. D4T (100 μM) did not reduce *Alu* RNA levels (normalized to u6 RNA). Fold change in densitometry compared to mock at 1 hr. *Alu* RNA-transfected cells in culture assayed at 24 hours for western blotting (Fig. 1, C and D, fig. S2A).

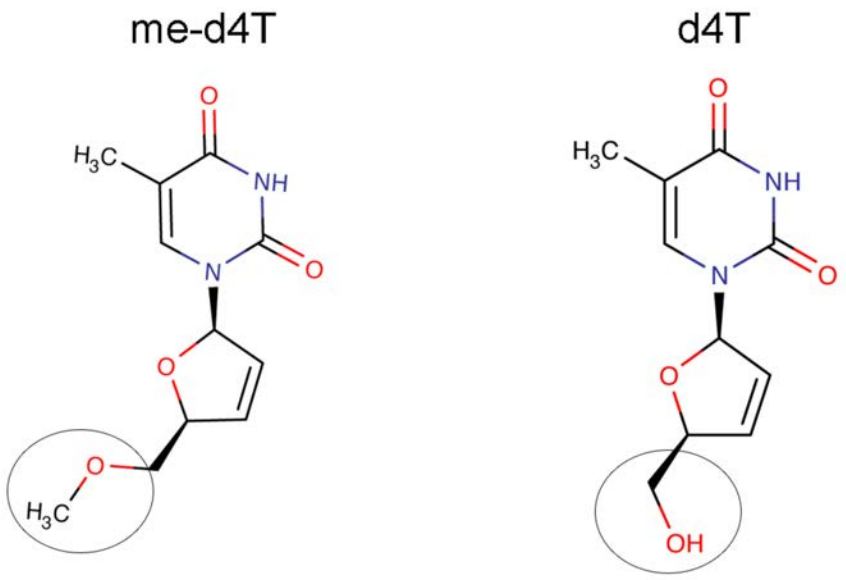

fig. S3. Chemical structure of me-d4T, related to Figure 2.

A single substitution of the ribose 5' hydroxyl group with a methoxy group (circled) designed to prevent d4T phosphorylation. See figs. S4 and S5 for detailed synthesis information.

A

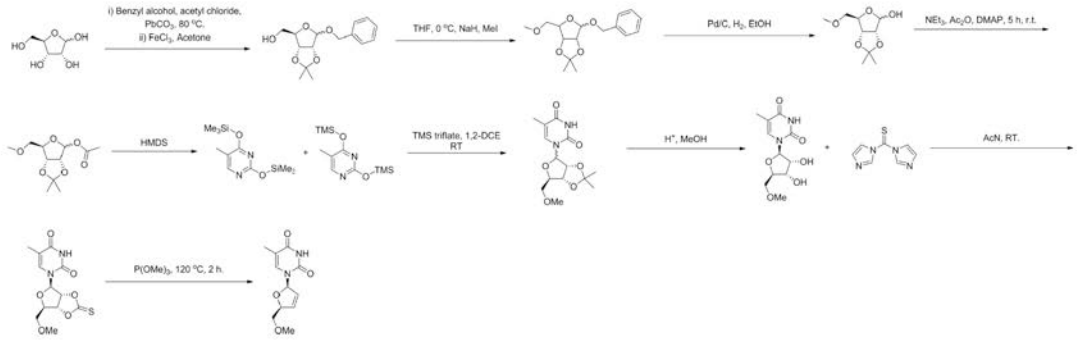

B

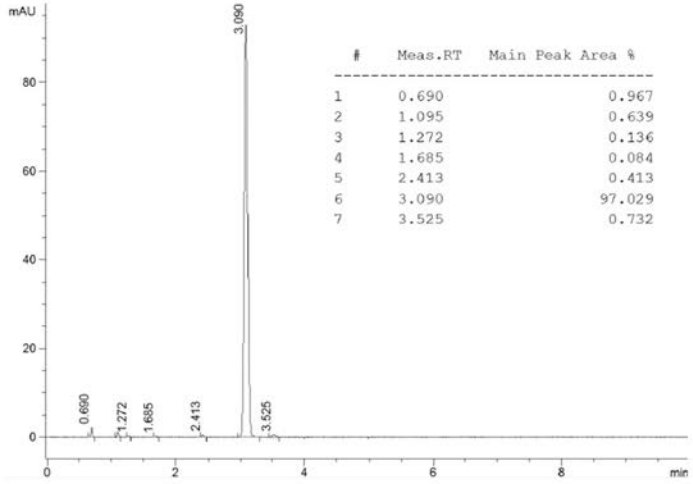

#	Meas.RT	Main Peak Area %
1	0.690	0.967
2	1.095	0.639
3	1.272	0.136
4	1.685	0.084
5	2.413	0.413
6	3.090	97.029
7	3.525	0.732

fig. S4. Synthesis of me-d4T, related to Figure 2.

(A) Schematic overview of me-d4T synthesis.

(B) HPLC chromatogram of me-d4T (peak # 6) final product, >97% purity.

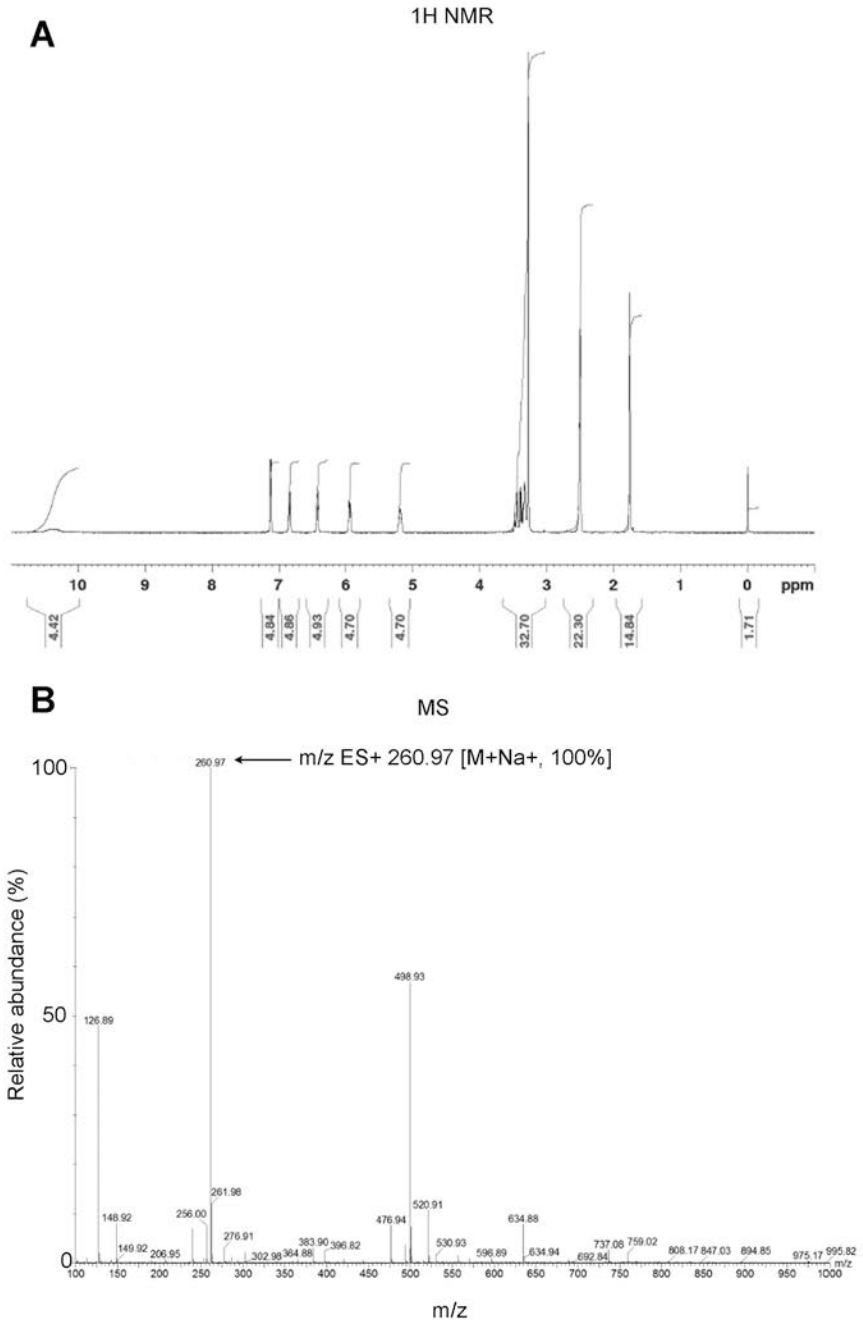

fig. S5. Synthesis of me-d4T, related to Figure 2.

(A) 1H NMR spectroscopy of me-d4T final product, chemical shifts consistent with structure.

(B) Liquid chromatography/mass spectrometry of me-d4T final product, m/z ratio consistent with structure.

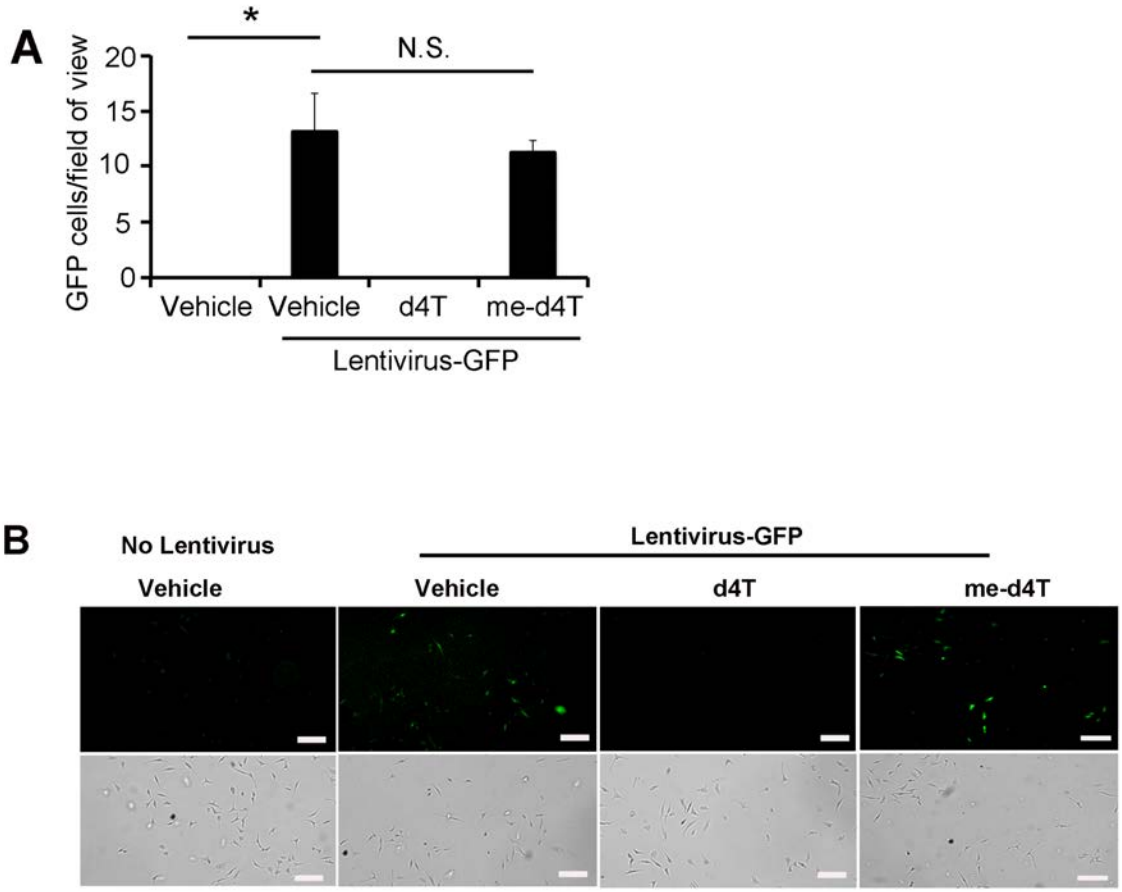

fig. S6. Lentiviral vector transduction of GFP, related to Figure 2.

Lentiviral vector transduction of GFP in HeLa cells treated with unmodified d4T or me-d4T (100 μM both drugs). **(A)** Quantification of GFP-positive cells per field of view, n = 4, * $P < 0.05$ by one-way ANOVA and Tukey's post-hoc test. Error bars S.E.M. **(B)** Representative images. Scale bars 200 μm.

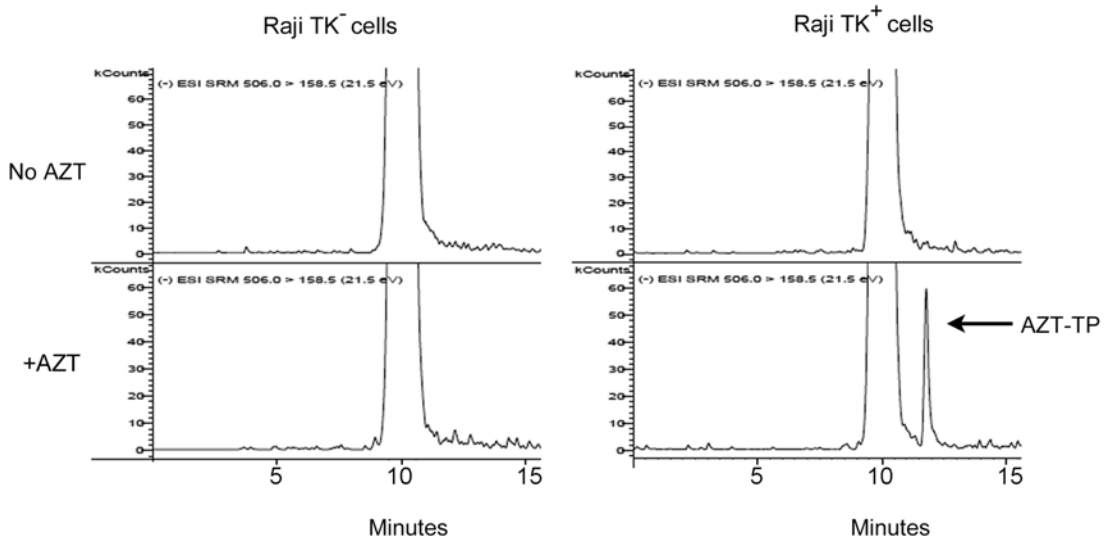

fig. S7. LC-MS/MS of AZT-TP, related to Figure 3.

Liquid chromatography-mass spectrometry (LC-MS) of Raji TK^+ cells and Raji TK^- cells treated with AZT (100 μM). Arrow in chromatogram points to peak for AZT-triphosphate (AZT-TP).

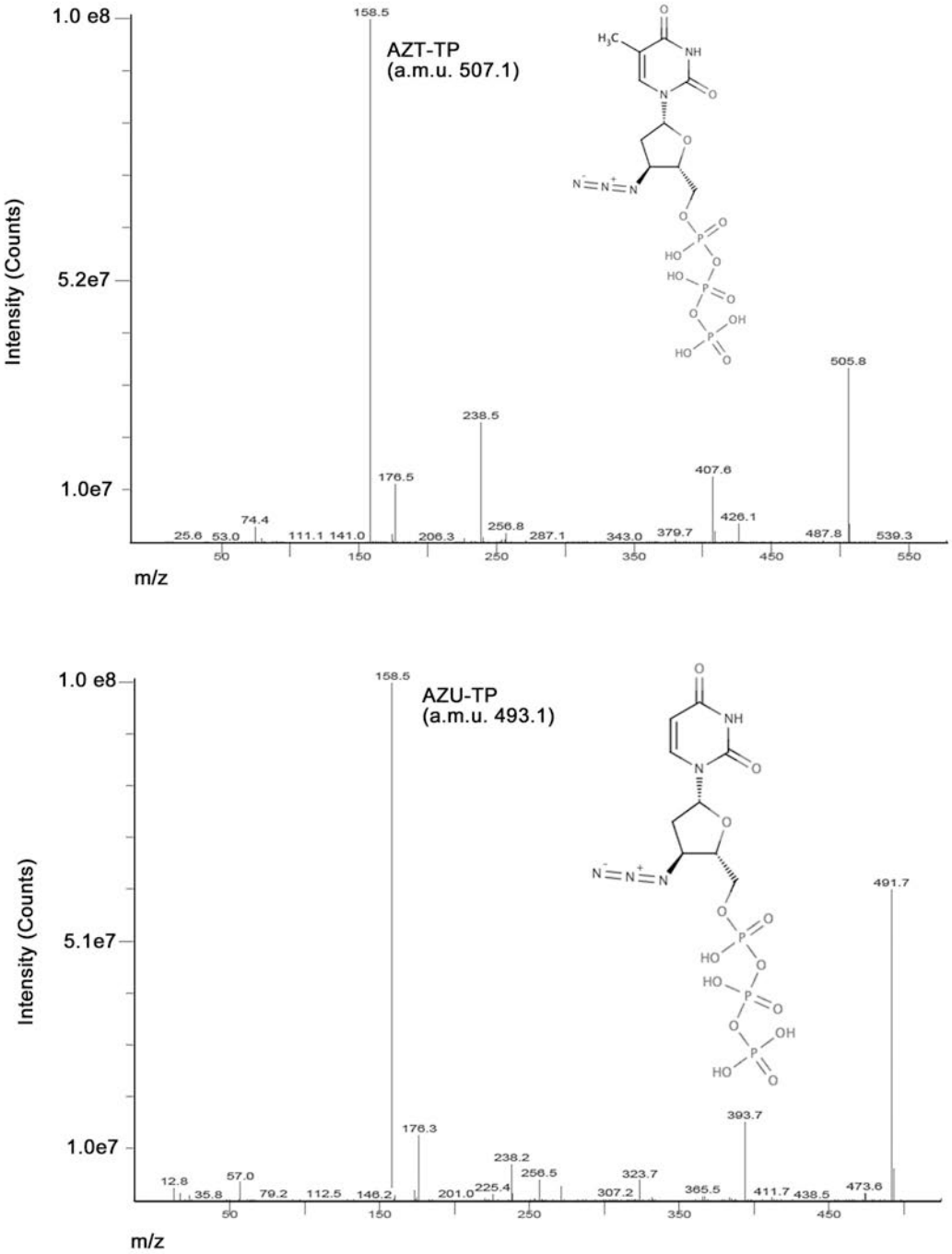

fig. S8. LC-MS/MS of AZT-TP and AZU-TP, related to Figure 3.

LC-MS/MS spectra of AZT-triphosphate (AZT-TP, target compound; top) and AZU-triphosphate (AZU-TP, internal standard; bottom).

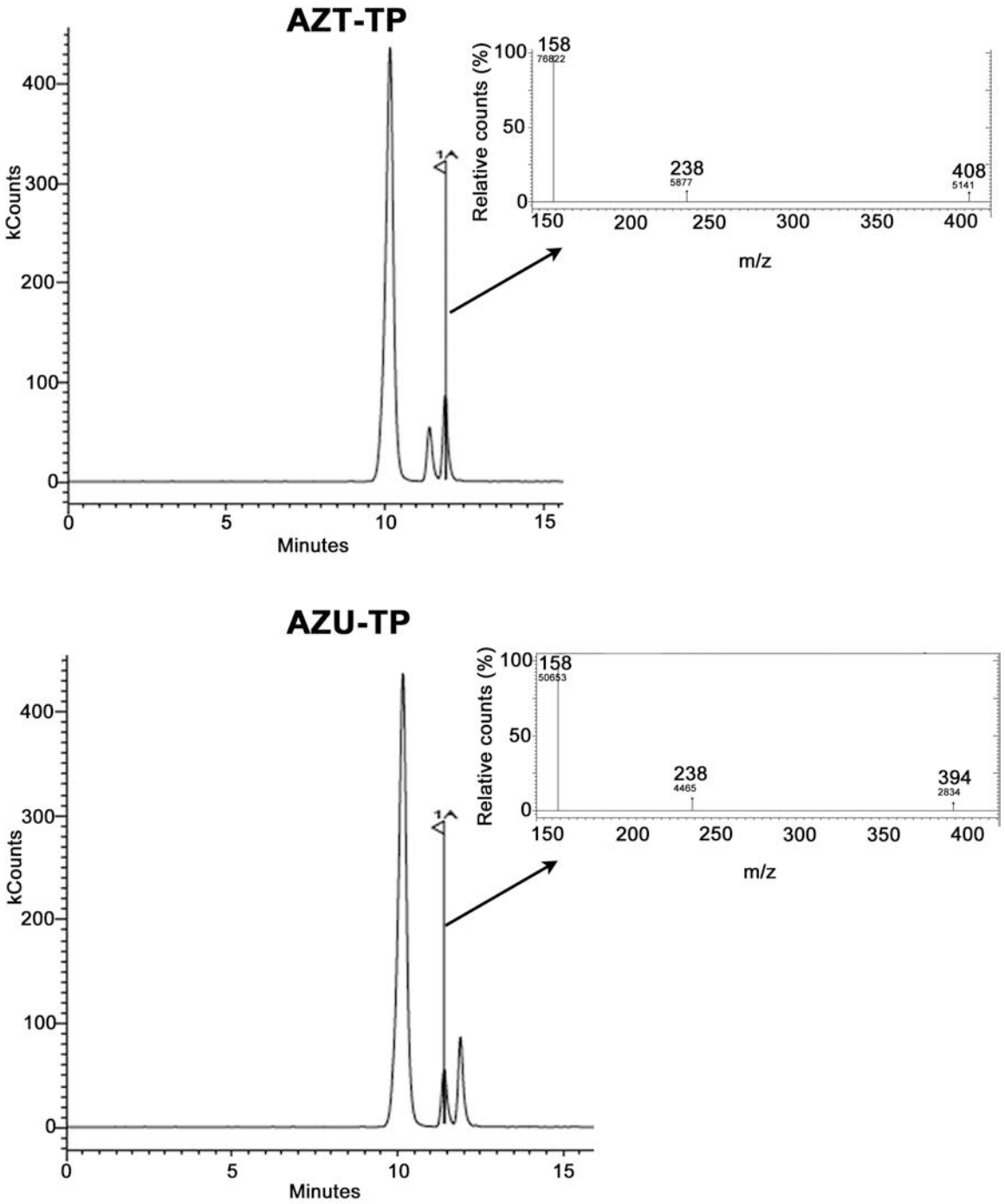

fig. S9. AZT-TP and AZU-TP separation by liquid chromatography.

Chromatographic separation of Raji TK$^-$ cells spiked with AZT-TP (top) and AZU-TP (bottom) with MS spectra (insets) to confirm identity of designated peaks.

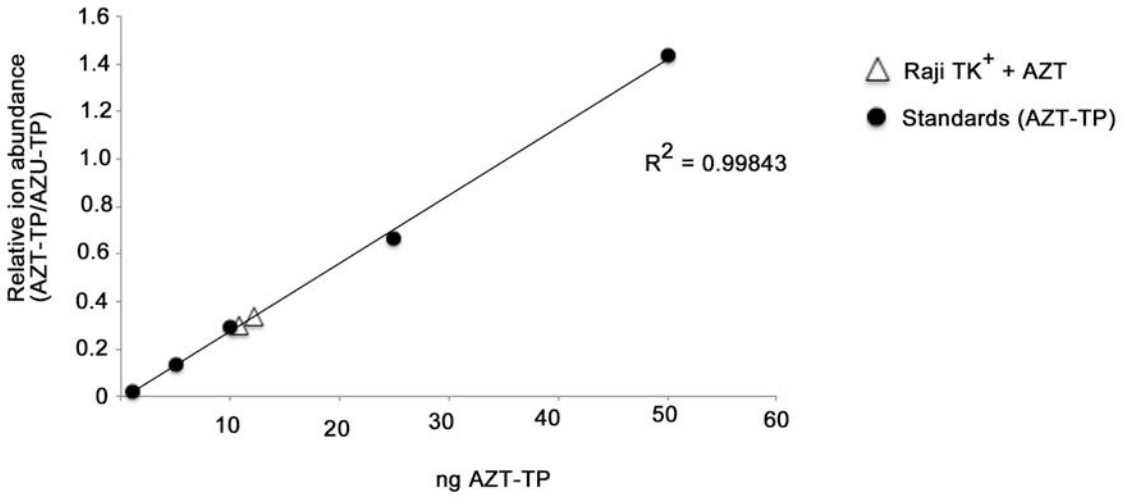

fig. S10. AZT-TP formation in Raji TK$^+$ cells.

Standard curve of AZT-TP standards (black circle). Raji TK$^+$ samples treated with AZT (100 μM) produced AZT-TP (white triangles), whereas AZT-TP was not detectable in Raji TK$^-$ cells treated with AZT. Representative of two experiments.

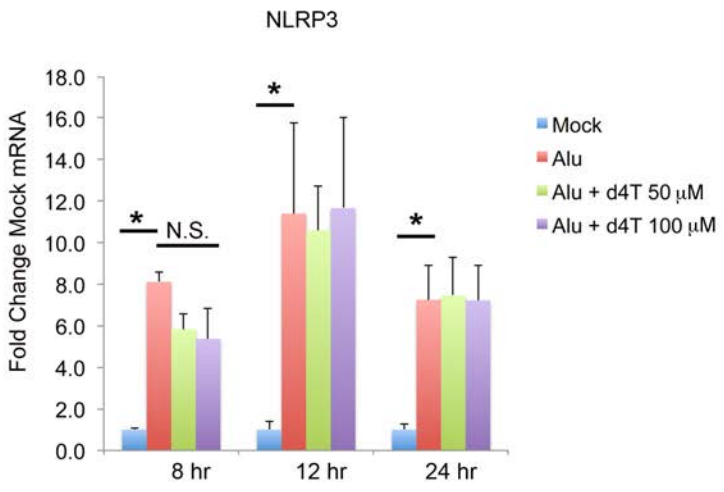

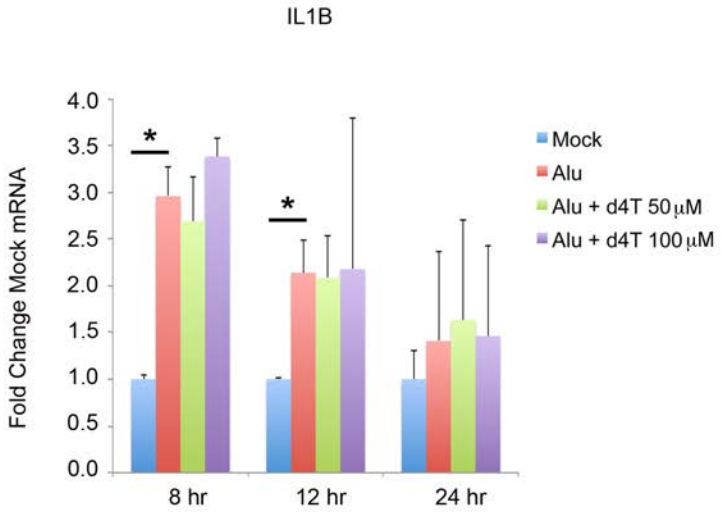

fig. S11. d4T does not inhibit *Alu*-induced inflammasome priming. Real time qRT-PCR of inflammasome genes (NLRP3- Top; IL1B- Bottom) after *Alu* RNA transfection in primary human RPE cells with or without d4T (50 or 100 μM). Top: NLRP3; Bottom: IL1B. n = 4, * $P < 0.05$ by one-way ANOVA and Tukey's post-hoc test, error bars S.E.M, N.S. = not significant.

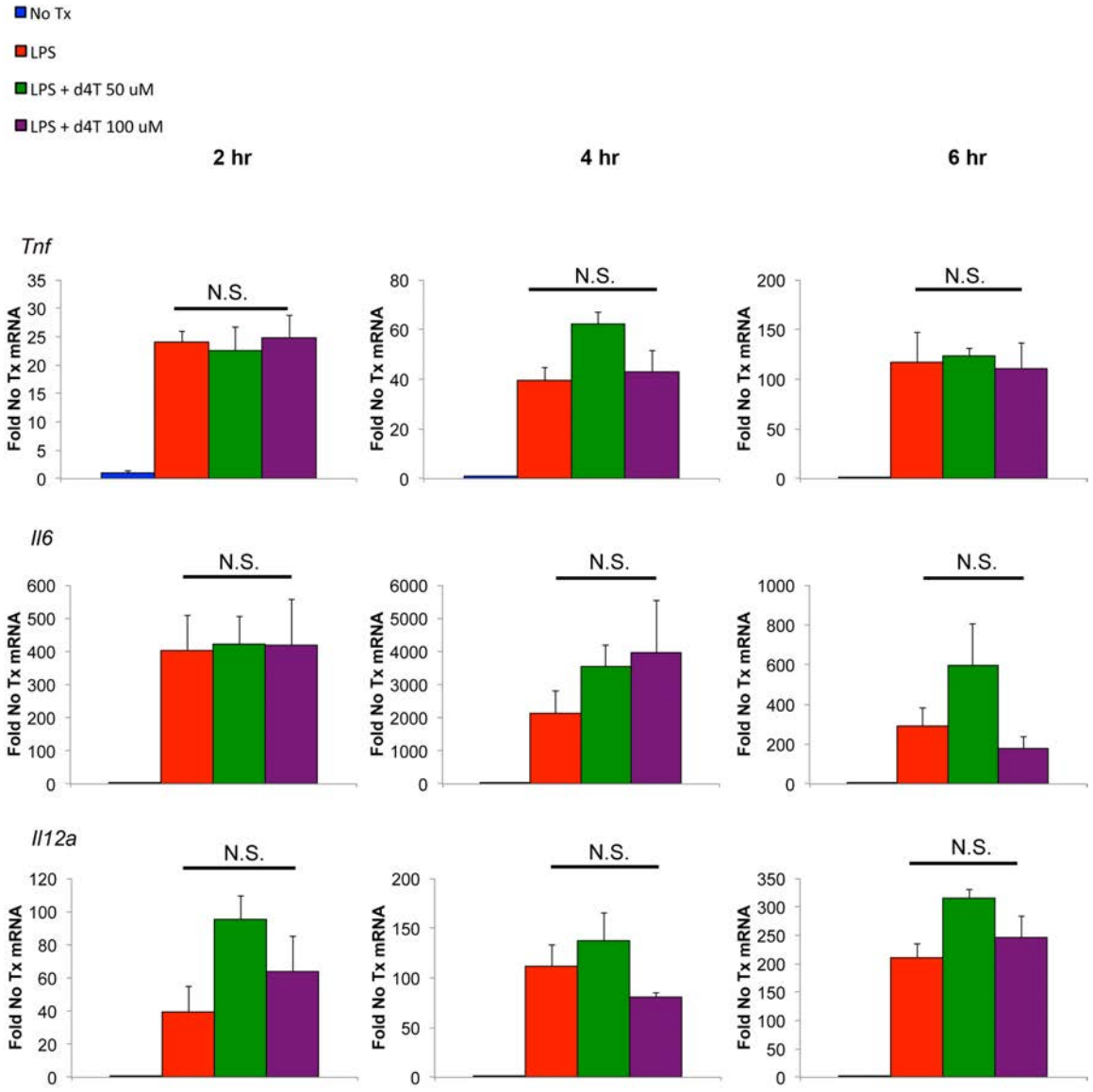

fig. S12. d4T does not inhibit LPS-induced mRNA expression of *Il6, Il12, Tnfa.*

Primary mouse bone marrow-derived macrophages were incubated with LPS with or without d4T (50 or 100 μM) and expression of *Il6, Il12a,* and *Tnf* mRNAs was monitored by real-time quantitative PCR at 2, 4 and 6 hours. N.S. = not significant by one-way ANOVA, error bars S.E.M.

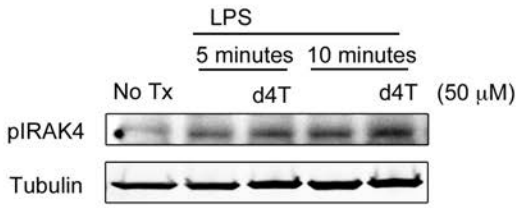

fig. S13. d4T does not inhibit LPS-induced IRAK4 phosphorylation in BMDMs. Primary mouse bone marrow-derived macrophages were incubated with LPS with or without d4T (50 μM) and samples were collected 5 or 10 minutes after addition of LPS. Representative of n = 3 experiments.

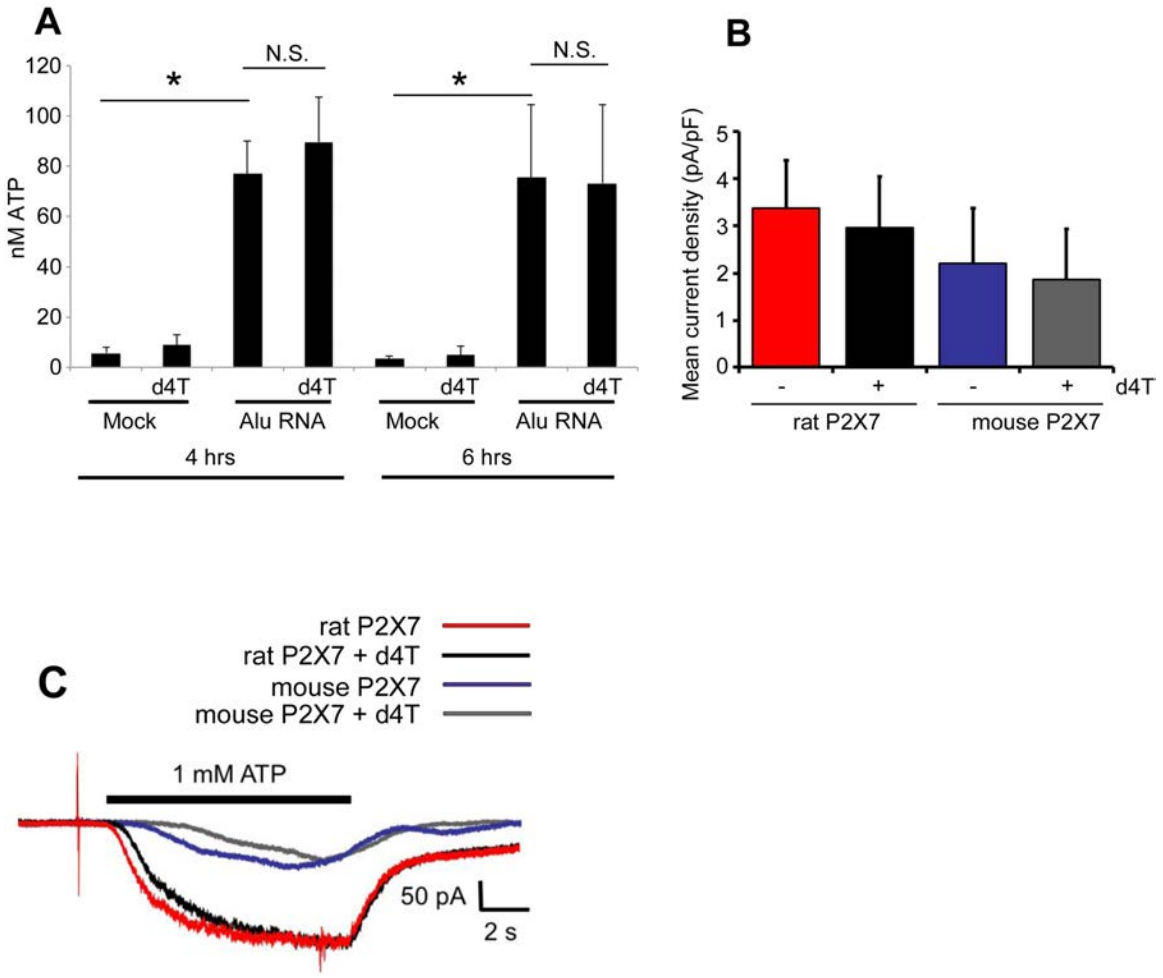

fig. S14. d4T does not block ATP release or P2X7 cation function.

(A) *Alu*-induced ATP release from primary human RPE cells treated with d4T (100 μM) (n = 4). **(B, C)** Whole-cell patch clamp of rat and mouse P2X7 receptors in HEK293 cells. Cells were pre-incubated in d4T for at least 1 minute prior to application of 1 mM ATP (also in the presence of d4T). Currents were recorded in solutions containing low concentrations of divalent cations (giving larger currents but causing delayed return of current to baseline after washout). **(B)** Histogram showing the mean current density

recorded for rat P2X7 and mouse P2X7 in the absence (–) and presence (+) of 100 μM d4T. Error bars represent standard error of the mean (n = 6 for rat P2X7 and n = 3 for mouse P2X7). No significant difference to recorded currents was observed in the presence of d4T. **(C)** Representative current traces from rat P2X7 in the absence (red) and presence (black) and mouse P2X7 in the absence (blue) and presence (grey) of 100 μM d4T. (A) * $p < 0.05$ by one-way ANOVA and Tukey's post-hoc test, N.S. not significant. (A) and (B) error bars S.E.M.

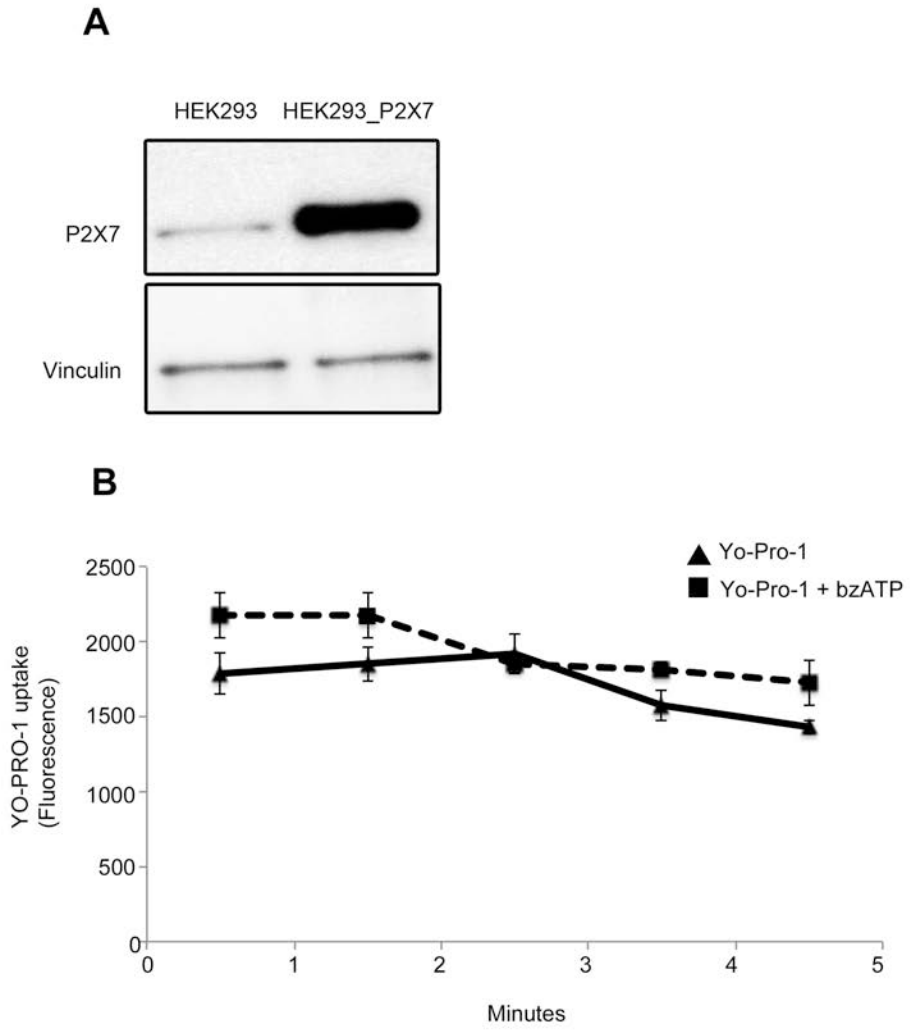

fig. S15. bzATP induces P2X7-dependent YO-PRO-1 uptake. (A) Western blot for P2X7 in HEK293 cells vs. HEK293 cells stably expressing the human P2X7 receptor. (B) YO-PRO-1 uptake (fluorescence) in P2X7-deficient HEK293 cells after addition of bzATP. n= 3. Error bars S.E.M.

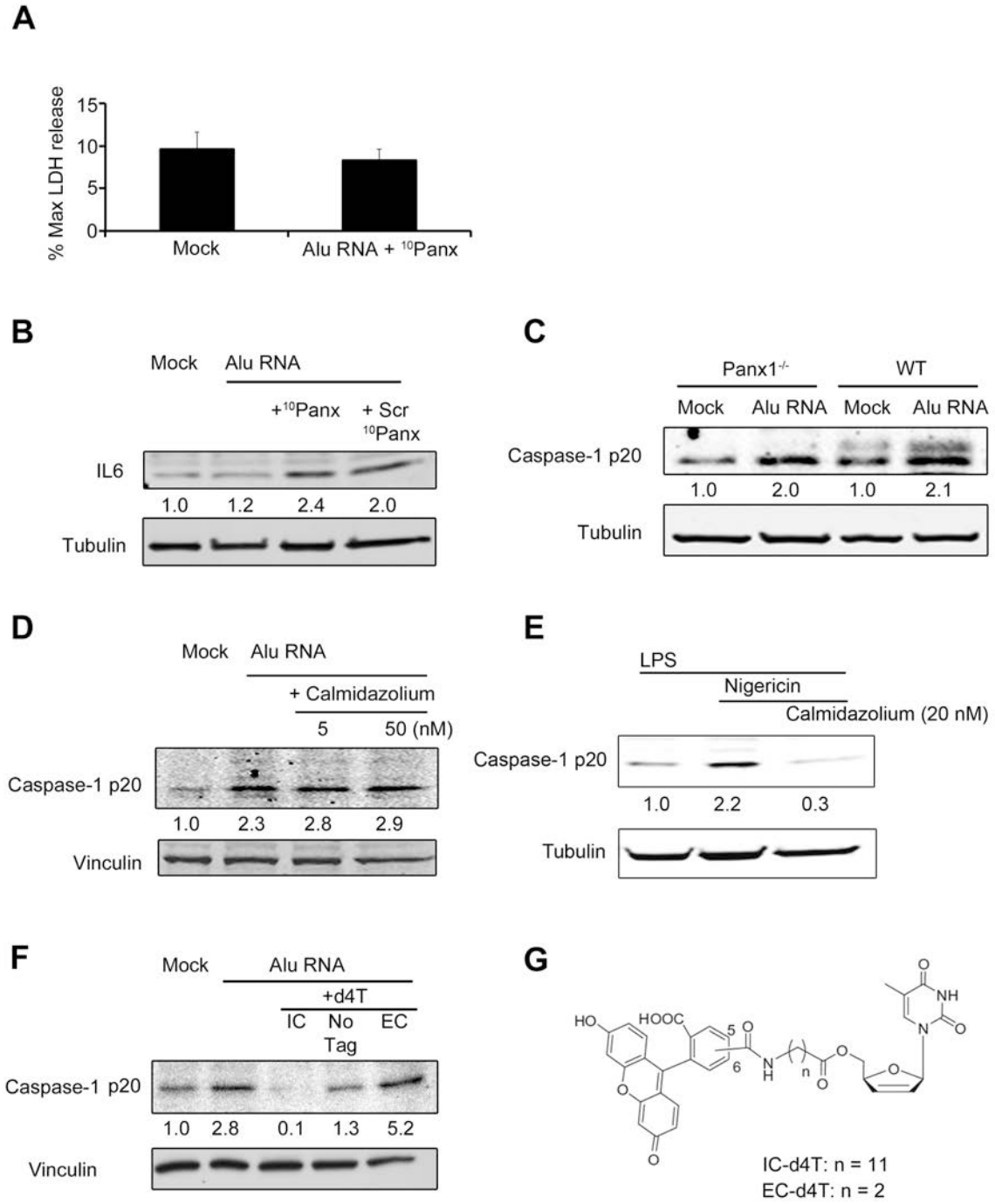

fig. S16. P2X7-dependent pore function mediates *Alu*-induced Caspase-1 activation.

(A) LDH levels in cell culture media of ^{10}Panx-treated cells compared to mock-treated cells + vehicle (samples from Fig. 4A experiment). Representative of n = 3 experiments. N.S. not significant by Student's t-test. Error bars S.E.M.

(B) Western blot showing that primary human RPE cells were still capable of synthesizing IL-6 after treatment with ^{10}Panx. Representative of n = 3 experiments.

(C) Western blot for Caspase-1 activation (p20) in primary mouse RPE cells from mice lacking the Pannexin-1 gene (*Panx1*) or wild-type mice with mock or *Alu* RNA transfection. Representative of n = 3 experiments. Fold change in densitometry compared to mock.

(D) Western blot of Caspase-1 activation (p20) in primary human RPE cells treated with *Alu* RNA $\pm$ calmidazolium (5 or 50 nM), which blocks P2X7 cation flux but not pore function. Representative of n = 3 experiments. Fold change in densitometry compared to mock.

(E) Western blot of Caspase-1 activation (p20) in primary human RPE cells treated with LPS/nigericin $\pm$ calmidazolium (20 nM). Representative of n = 3 experiments. Fold change in densitometry compared to LPS alone.

(F) Western blot of Caspase-1 activation (p20) in primary human RPE cells transfected with *Alu* RNA $\pm$ cell permeable (IC), unmodified (no tag) d4T, or cell-impermeable (EC) d4T. All drugs administered at 100 μM. Representative of n = 3 experiments. Fold change in densitometry compared to mock.

(G) Chemical structure of IC- and EC-d4T used in (F).

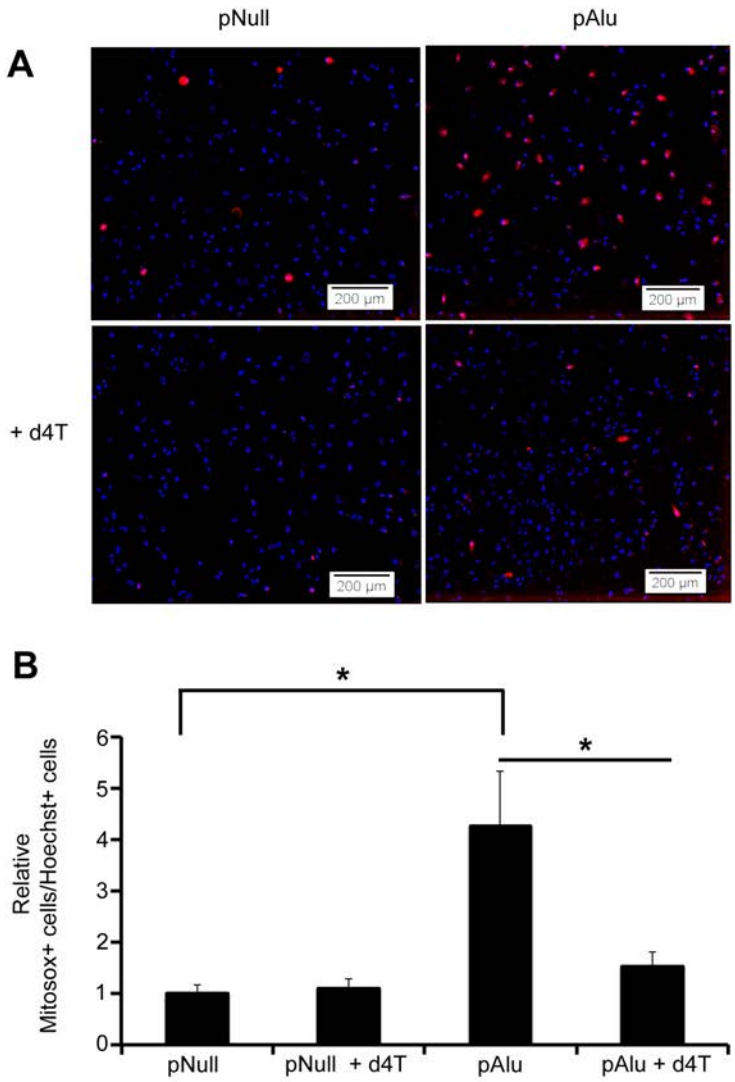

fig. S17. d4T blocks *Alu*-induced mtROS production.

(A) Mitochondrial ROS visualized with MitoSox (Red) and cell nuclei with Hoechst (Blue) in primary human RPE cells transfected with pNull or pAlu $\pm$ d4T (100 µM). Representative image of n = 3-4.

(B) Quantification of images from experiment in fig. S17A (Relative $MitoSOx^{+}/Hoechst^{+}$ cells). * $P < 0.05$ by one-way ANOVA and Tukey's post-hoc test. n = 3-4, error bars S.E.M.

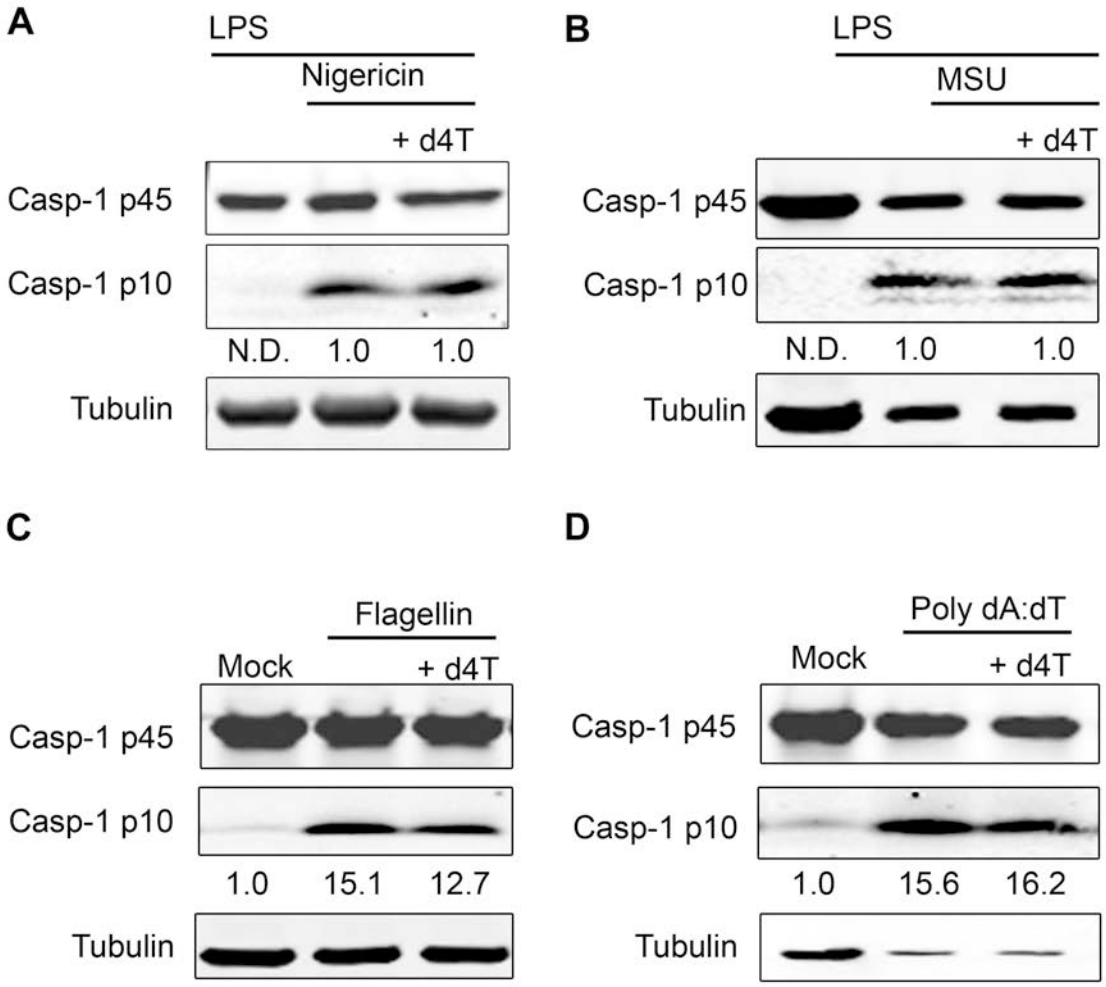

fig. S18. d4T does not inhibit P2X7-independent NLRP3 inflammasome nor AIM2/NLRC4 inflammasomes.

Western blot of pro-Caspase-1 (p45) or active Caspase-1 (p10) from primary bone marrow-derived macrophages with d4T treatment (50 μM) and stimulation with (A) Nigericin (20 μM); (B) MSU (250 ug/mL); (C) Flagellin from *Salmonella* (20 μg/mL); (D) Poly dA:dT (1.5 μg/mL). A-D: n = 3-4. A,C,D: Active Caspase-1 detected in cell lysates; B: Active Caspase-1 detected in media (not detectable in cell lysate; not shown). N.D. not detectable. Fold change in densitometry compared to LPS alone (A and B) or mock transfected (C and D).

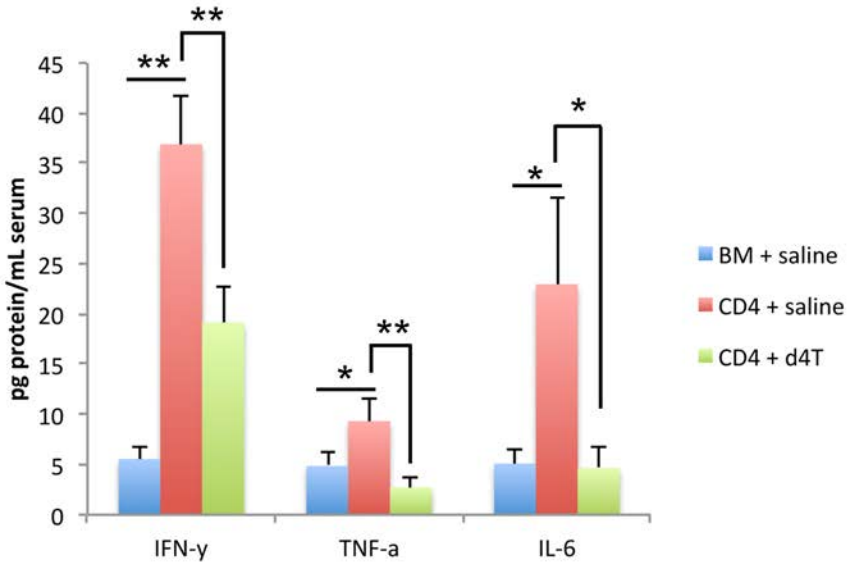

fig. S19. d4T reduces serum levels of IFN-γ, TNF-α, and IL6 in a murine model of acute graft-versus-host disease. Bone marrow transplants (C57Bl/6 into Balb/C mice) and intraperitoneal injections (starting on day –1; d4T or saline) were performed as in Fig. 4C. Serum was collected on day 3 after transplant and assayed for IFN-γ, TNF-α, and IL-6 proteins by Luminex assay. * $P < 0.05$; ** $P < 0.01$ by one-way ANOVA and Tukey's post-hoc test. n = 9–10 mice/group, error bars S.E.M.

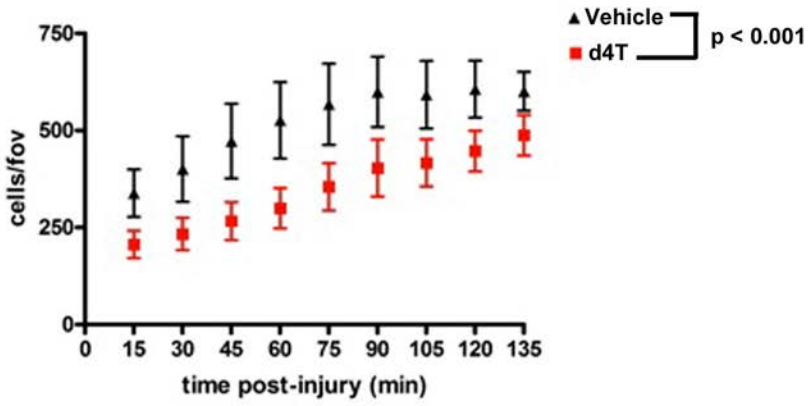

fig. S20. d4T inhibits neutrophil chemotaxis after acute liver injury.

LysMeGFP cells/FOV around a sterile focal hepatic lesion. d4T (400 mg/kg) or PBS administered via jugular vein 20 minutes prior to injury. n = 4, error bars S.E.M., $P < 0.001$ between groups vehicle vs. d4T by two-way ANOVA.

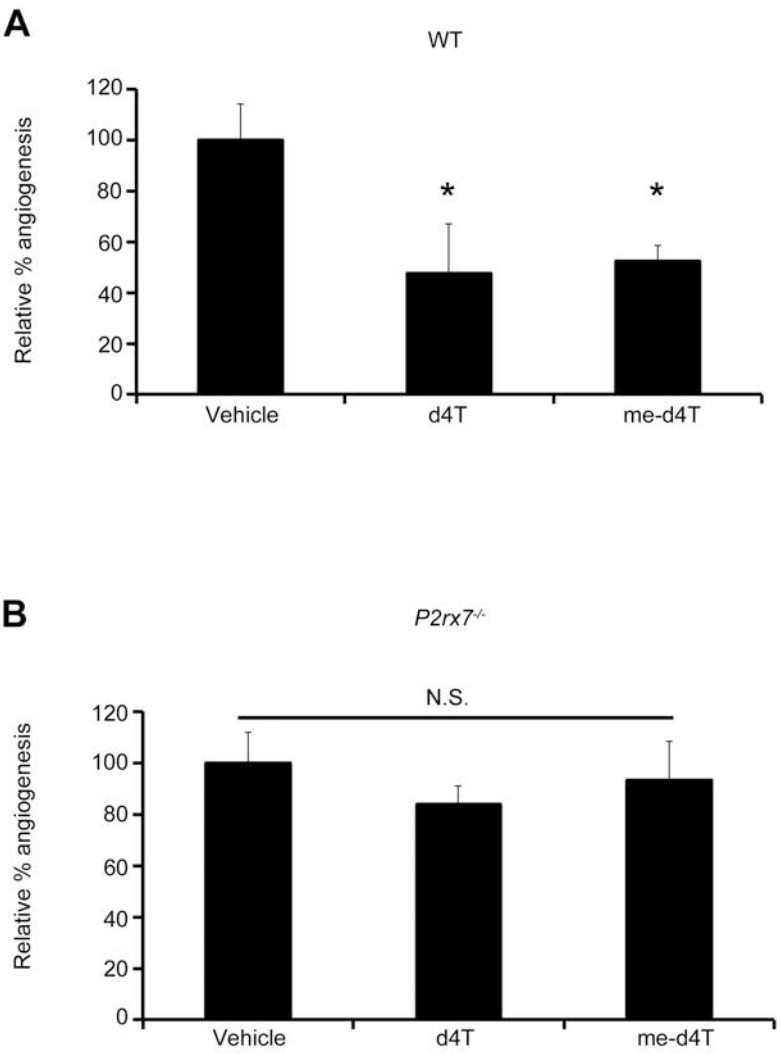

fig. S21. d4T and me-d4T inhibit choroidal neovascularization.

Laser-induced choroidal neovascularization in (A) wild-type mice and (B) *P2rx7*$^{-/-}$ mice treated with d4T (125 ng) and me-d4T (62.5 ng). Volumes normalized to vehicle treatment and expressed as relative % angiogenesis. * P <0.05 by one-way ANOVA and Tukey's post-hoc test, n = 10-12, error bars S.E.M. N.S., not significant.